СТАНДАРНАЯ КОСМОЛОГИЧЕСКАЯ МОДЕЛЬ

SCM

$\Lambda CDM + (k=0) + (n_s = 1)_{ad}$

$\Omega_m \approx 0.3$

$\Omega_\Lambda \approx 0.7$

Точность: ~ 10%

$H_0 = 72 \pm 7$ км/с/Мпс $\quad (60 < H_0 < 80)$

- ОПРЕДЕЛЯЕТ СОВРЕМЕННЫЙ МОМЕНТ

4 ОСНОВНЫХ КОСМОЛОГИЧЕСКИХ ПОСТОЯННЫХ

1. $\frac{n_b}{n_\gamma} = 5.98 \cdot 10^{-10} \cdot \frac{\Omega_b h^2}{0.022} \cdot \left(\frac{2.73}{T_\gamma}\right)^3$

$h = \frac{H_0}{100}$

2. $\frac{\varepsilon_b}{\varepsilon_m} = \frac{\varepsilon_b}{\varepsilon_b + \varepsilon_{CDM}} = 0.150 \cdot \frac{\Omega_b h^2}{0.022} \cdot \frac{0.3}{\Omega_m}$

3. $\frac{G^2 \hbar \varepsilon_\Lambda}{c^7} = 1.25 * 10^{-123} \cdot \frac{\Omega_\Lambda}{0.7} \cdot \left(\frac{h}{0.7}\right)^2 \cdot \frac{6.673 \cdot 10^{-8}}{G}$

$\rho_\Lambda = 6.44 \cdot 10^{-30} \cdot (\ldots\ldots)$ г·см$^{-3}$

4. $\tilde{A} = 2.92 \cdot 10^{-5} \cdot \left(\frac{A_{WMAP}}{0.8}\right)^{1/2} e^{\tau - 0.17}$

$\langle \Phi^2_{in} \rangle = \tilde{A}^2 \int \frac{dk}{k}$

НА СТАДИИ ДОМИНИРОВАНИЯ МАТЕРИИ

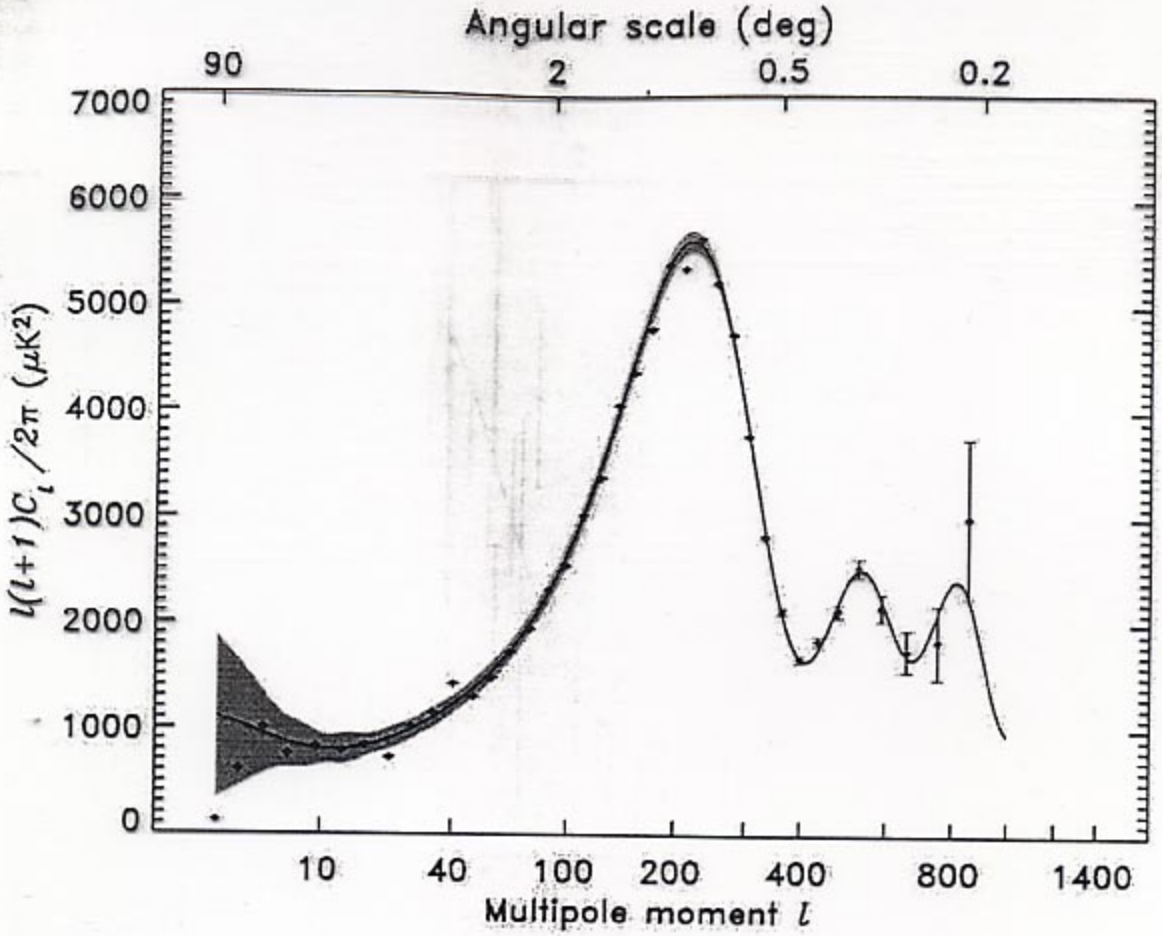

Fig. 8.— The final angular power spectrum, $l(l+1)C_l/2\pi$, obtained from the 28 cross-power spectra, as described in §5. The data are plotted with 1σ measurement errors only which reflect the combined uncertainty due to noise, beam, calibration, and source subtraction uncertainties. The solid line shows the best-fit ΛCDM model from Spergel et al. (2003). The grey band around the model is the 1σ uncertainty due to cosmic variance on the cut sky. For this plot, both the model and the error band have been binned with the same boundaries as the data, but they have been plotted as a splined curve to guide the eye. On the scale of this plot the unbinned model curve would be virtually indistinguishable from the binned curve except in the vicinity of the third peak.

Astronomy & Astrophysics manuscript no. Cl˙letter
(DOI: will be inserted by hand later)

AA 399, L19 (2003) March 14

The Cosmic Microwave Background Anisotropy Power Spectrum measured by Archeops

A. Benoît[1], P. Ade[2], A. Amblard[3,24], R. Ansari[4], É. Aubourg[5,24], S. Bargot[4], J. G. Bartlett[3,24], J.–Ph. Bernard[7,16], R. S. Bhatia[8], A. Blanchard[6], J. J. Bock[8,9], A. Boscaleri[10], F. R. Bouchet[11], A. Bourrachot[4], P. Camus[1], F. Couchot[4], P. de Bernardis[12], J. Delabrouille[3,24], F.–X. Désert[13], O. Doré[11], M. Douspis[6,14], L. Dumoulin[15], X. Dupac[16], P. Filliatre[17], P. Fosalba[11], K. Ganga[18], F. Gannaway[2], B. Gautier[1], M. Giard[16], Y. Giraud–Héraud[3,24], R. Gispert[7†⋆], L. Guglielmi[3,24], J.–Ch. Hamilton[3,17], S. Hanany[19], S. Henrot–Versillé[4], J. Kaplan[3,24], G. Lagache[7], J.–M. Lamarre[7,25], A. E. Lange[8], J. F. Macías–Pérez[17], K. Madet[1], B. Maffei[2], Ch. Magneville[5,24], D. P. Marrone[19], S. Masi[12], F. Mayet[5], A. Murphy[20], F. Naraghi[17], F. Nati[12], G. Patanchon[3,24], G. Perrin[17], M. Piat[7], N. Ponthieu[17], S. Prunet[11], J.–L. Puget[7], C. Renault[17], C. Rosset[3,24], D. Santos[17], A. Starobinsky[21], I. Strukov[22], R. V. Sudiwala[2], R. Teyssier[11,23], M. Tristram[17], C. Tucker[2], J.–C. Vanel[3,24], D. Vibert[11], E. Wakui[2], and D. Yvon[5,24]

[1] Centre de Recherche sur les Très Basses Températures, BP166, 38042 Grenoble Cedex 9, France
[2] Cardiff University, Physics Department, PO Box 913, 5, The Parade, Cardiff, CF24 3YB, UK
[3] Physique Corpusculaire et Cosmologie, Collège de France, 11 pl. M. Berthelot, F-75231 Paris Cedex 5, France
[4] Laboratoire de l'Accélérateur Linéaire, BP 34, Campus Orsay, 91898 Orsay Cedex, France
[5] CEA-CE Saclay, DAPNIA, Service de Physique des Particules, Bat 141, F-91191 Gif sur Yvette Cedex, France
[6] Laboratoire d'Astrophysique de l'Obs. Midi-Pyrénées, 14 Avenue E. Belin, 31400 Toulouse, France
[7] Institut d'Astrophysique Spatiale, Bât. 121, Université Paris XI, 91405 Orsay Cedex, France
[8] California Institute of Technology, 105-24 Caltech, 1201 East California Blvd, Pasadena CA 91125, USA
[9] Jet Propulsion Laboratory, 4800 Oak Grove Drive, Pasadena, California 91109, USA
[10] IROE–CNR, Via Panciatichi, 64, 50127 Firenze, Italy
[11] Institut d'Astrophysique de Paris, 98bis, Boulevard Arago, 75014 Paris, France
[12] Gruppo di Cosmologia Sperimentale, Dipart. di Fisica, Univ. "La Sapienza", P. A. Moro, 2, 00185 Roma, Italy
[13] Laboratoire d'Astrophysique, Obs. de Grenoble, BP 53, 38041 Grenoble Cedex 9, France
[14] Nuclear and Astrophysics Laboratory, Keble Road, Oxford, OX1 3RH, UK
[15] CSNSM–IN2P3, Bât 108, 91405 Orsay Campus, France
[16] Centre d'Étude Spatiale des Rayonnements, BP 4346, 31028 Toulouse Cedex 4, France
[17] Institut des Sciences Nucléaires, 53 Avenue des Martyrs, 38026 Grenoble Cedex, France
[18] Infrared Processing and Analysis Center, Caltech, 770 South Wilson Avenue, Pasadena, CA 91125, USA
[19] School of Physics and Astronomy, 116 Church St. S.E., University of Minnesota, Minneapolis MN 55455, USA
[20] Experimental Physics, National University of Ireland, Maynooth, Ireland
[21] Landau Institute for Theoretical Physics, 119334 Moscow, Russia
[22] Space Research Institute, Profsoyuznaya St. 84/32, Moscow, Russia
[23] CEA-CE Saclay, DAPNIA, Service d'Astrophysique, Bat 709, F-91191 Gif sur Yvette Cedex, France
[24] Fédération de Recherche APC, Université Paris 7, Paris, France
[25] LERMA, Observatoire de Paris, 61 Av. de l'Observatoire, 75014 Paris, France

Received 16 October 2002/Accepted 15 December 2002

Abstract. We present a determination by the Archeops experiment of the angular power spectrum of the cosmic microwave background anisotropy in 16 bins over the multipole range $\ell = 15 - 350$. Archeops was conceived as a precursor of the Planck HFI instrument by using the same optical design and the same technology for the detectors and their cooling. Archeops is a balloon–borne instrument consisting of a 1.5 m aperture diameter telescope and an array of 21 photometers maintained at ~ 100 mK that are operating in 4 frequency bands centered at 143, 217, 353 and 545 GHz. The data were taken during the Arctic night of February 7, 2002 after the instrument was launched by CNES from Esrange base (Sweden). The entire data cover ~ 30% of the sky. This first analysis was obtained with a small subset of the dataset using the most sensitive photometer in each CMB band (143 and 217 GHz) and 12.6% of the sky at galactic latitudes above 30 degrees where the foreground contamination is measured to be negligible. The large sky coverage and medium resolution (better than 15 arcmin.) provide for the first time a high signal-to-noise ratio determination of the power spectrum over angular scales that include both the first acoustic peak and scales probed by COBE/DMR. With a binning of $\Delta\ell$=7 to 25 the error bars are dominated by sample variance for ℓ below 200. A companion paper details the cosmological implications.

Key words. Cosmic microwave background – Cosmology: observations – Submillimeter

Astronomy & Astrophysics manuscript no. CParam˙letter
(DOI: will be inserted by hand later)

AA 399, L25 February 22 (2003)

Cosmological constraints from Archeops

A. Benoît[1], P. Ade[2], A. Amblard[3,24], R. Ansari[4], É. Aubourg[5,24], S. Bargot[4], J. G. Bartlett[3,24], J.–Ph. Bernard[7,16], R. S. Bhatia[8], A. Blanchard[6], J. J. Bock[8,9], A. Boscaleri[10], F. R. Bouchet[11], A. Bourrachot[4], P. Camus[1], F. Couchot[4], P. de Bernardis[12], J. Delabrouille[3,24], F.–X. Désert[13], O. Doré[11], M. Douspis[6,14], L. Dumoulin[15], X. Dupac[16], P. Filliatre[17], P. Fosalba[11], K. Ganga[18], F. Gannaway[2], B. Gautier[1], M. Giard[16], Y. Giraud–Héraud[3,24], R. Gispert[7†⋆], L. Guglielmi[3,24], J.–Ch. Hamilton[3,17], S. Hanany[19], S. Henrot–Versillé[4], J. Kaplan[3,24], G. Lagache[7], J.–M. Lamarre[7,25], A. E. Lange[8], J. F. Macías–Pérez[17], K. Madet[1], B. Maffei[2], Ch. Magneville[5,24], D. P. Marrone[19], S. Masi[12], F. Mayet[5], A. Murphy[20], F. Naraghi[17], F. Nati[12], G. Patanchon[3,24], G. Perrin[17], M. Piat[7], N. Ponthieu[17], S. Prunet[11], J.–L. Puget[7], C. Renault[17], C. Rosset[3,24], D. Santos[17], A. Starobinsky[21], I. Strukov[22], R. V. Sudiwala[2], R. Teyssier[11,23], M. Tristram[17], C. Tucker[2], J.–C. Vanel[3,24], D. Vibert[11], E. Wakui[2], and D. Yvon[5,24]

[1] Centre de Recherche sur les Très Basses Températures, BP166, 38042 Grenoble Cedex 9, France
[2] Cardiff University, Physics Department, PO Box 913, 5, The Parade, Cardiff, CF24 3YB, UK
[3] Physique Corpusculaire et Cosmologie, Collège de France, 11 pl. M. Berthelot, F-75231 Paris Cedex 5, France
[4] Laboratoire de l'Accélérateur Linéaire, BP 34, Campus Orsay, 91898 Orsay Cedex, France
[5] CEA-CE Saclay, DAPNIA, Service de Physique des Particules, Bat 141, F-91191 Gif sur Yvette Cedex, France
[6] Laboratoire d'Astrophysique de l'Obs. Midi-Pyrénées, 14 Avenue E. Belin, 31400 Toulouse, France
[7] Institut d'Astrophysique Spatiale, Bât. 121, Université Paris XI, 91405 Orsay Cedex, France
[8] California Institute of Technology, 105-24 Caltech, 1201 East California Blvd, Pasadena CA 91125, USA
[9] Jet Propulsion Laboratory, 4800 Oak Grove Drive, Pasadena, California 91109, USA
[10] IROE–CNR, Via Panciatichi, 64, 50127 Firenze, Italy
[11] Institut d'Astrophysique de Paris, 98bis, Boulevard Arago, 75014 Paris, France
[12] Gruppo di Cosmologia Sperimentale, Dipart. di Fisica, Univ. "La Sapienza", P. A. Moro, 2, 00185 Roma, Italy
[13] Laboratoire d'Astrophysique, Obs. de Grenoble, BP 53, 38041 Grenoble Cedex 9, France
[14] Nuclear and Astrophysics Laboratory, Keble Road, Oxford, OX1 3RH, UK
[15] CSNSM–IN2P3, Bât 108, 91405 Orsay Campus, France
[16] Centre d'Étude Spatiale des Rayonnements, BP 4346, 31028 Toulouse Cedex 4, France
[17] Institut des Sciences Nucléaires, 53 Avenue des Martyrs, 38026 Grenoble Cedex, France
[18] Infrared Processing and Analysis Center, Caltech, 770 South Wilson Avenue, Pasadena, CA 91125, USA
[19] School of Physics and Astronomy, 116 Church St. S.E., University of Minnesota, Minneapolis MN 55455, USA
[20] Experimental Physics, National University of Ireland, Maynooth, Ireland
[21] Landau Institute for Theoretical Physics, 119334 Moscow, Russia
[22] Space Research Institute, Profsoyuznaya St. 84/32, Moscow, Russia
[23] CEA-CE Saclay, DAPNIA, Service d'Astrophysique, Bat 709, F-91191 Gif sur Yvette Cedex, France
[24] Fédération de Recherche APC, Université Paris 7, Paris, France
[25] LERMA, Observatoire de Paris, 61 Av. de l'Observatoire, 75014 Paris, France

Received 16 October 2002/Accepted 22 November 2002

Abstract. We analyze the cosmological constraints that Archeops (Benoît et al. 2002) places on adiabatic cold dark matter models with passive power-law initial fluctuations. Because its angular power spectrum has small bins in ℓ and large ℓ coverage down to COBE scales, Archeops provides a precise determination of the first acoustic peak in terms of position at multipole $l_{\rm peak} = 220 \pm 6$, height and width. An analysis of Archeops data in combination with other CMB datasets constrains the baryon content of the Universe, $\Omega_b h^2 = 0.022^{+0.003}_{-0.004}$, compatible with Big-Bang nucleosynthesis and with a similar accuracy. Using cosmological priors obtained from recent non–CMB data leads to yet tighter constraints on the total density, *e.g.* $\Omega_{\rm tot} = 1.00^{+0.03}_{-0.02}$ using the HST determination of the Hubble constant. An excellent absolute calibration consistency is found between Archeops and other CMB experiments, as well as with the previously quoted best fit model. The spectral index n is measured to be $1.04^{+0.10}_{-0.12}$ when the optical depth to reionization, τ, is allowed to vary as a free parameter, and $0.96^{+0.03}_{-0.04}$ when τ is fixed to zero, both in good agreement with inflation.

Key words. Cosmic microwave background – Cosmological parameters – Early Universe – Large–scale structure of the Universe

МЕТРИКА ΛCM

$$ds^2 = dt^2 - a^2(t)\left(dx^2 + dy^2 + dz^2\right)$$

$$a(t) = a_0 \, sh^{2/3}\left(\frac{3}{2} H_\infty t\right) \qquad z \ll z_{eq}$$

$$H(t) \equiv \frac{\dot{a}}{a}$$ – ПАРАМЕТР ХАББЛА

$$H_\infty = H_0 \sqrt{1 - \Omega_m}$$

$$q(t) \equiv -\frac{\ddot{a}\, a}{\dot{a}^2} = \frac{3}{2}\Omega_m - 1$$ – ПАРАМЕТР ЗАМЕДЛЕНИЯ

$$\Omega_m(t) = \frac{8\pi G \varepsilon_m(t)}{3H^2(t)}$$

$$z(t) \equiv \frac{\dddot{a}\, a^2}{\dot{a}^3} = 1$$

ДРУГИЕ МАЛЫЕ ФУНДАМЕНТАЛЬНЫЕ ПАРАМЕТРЫ

5. Ω_ν

$$\Omega_\nu h^2 = \frac{\sum_i m_{\nu i}\,(eV)}{93.6} \cdot \left(\frac{T_\gamma}{2.73}\right)^3$$

$$10^{-3} \lesssim \Omega_\nu \lesssim 0.02 \qquad \sum_i m_{\nu i} < 1\ eV$$

6. $n_s - 1\ (k)$

ОЖИДАЕТСЯ: $|n_s - 1| \sim \frac{const}{N} \sim$ few %

ПОКА: $N = 50\text{-}60$

$|n_s - 1| \lesssim 0.1$

7. $\frac{dn_s}{d\ln k}\ (k)$

ОЖИДАЕТСЯ: $\left|\frac{dn_s}{d\ln k}\right| \sim |n_s - 1|^2 \sim 10^{-3}$

РЕЗУЛЬТАТ WMAP $\frac{dn_s}{d\ln k} \simeq -0.03$

НЕ ПОДТВЕРЖДЕН!

8–9. $r(k),\ n_T(k)$

$$r \equiv \left(\frac{C_{\ell 2}}{C_{\ell 5}}\right)_{10} < 0.4$$

НЕФУНДАМЕНТАЛЬНЫЕ ПАРАМЕТРЫ

10. $\tau = 0.1 - 0.2$

11. $b \equiv \left(\frac{\delta\rho}{\rho}\right)_{gal} \Big/ \left(\frac{\delta\rho}{\rho}\right)_{m} = 1.1 \pm 0.1$

КОСМОЛОГИЧЕСКИЕ "СОВПАДЕНИЯ"

1. $\varepsilon_m \sim \varepsilon_\Lambda$ "СЕЙЧАС"

$$\frac{t_0}{t_{Pl}} \sim \left(\frac{M_{Pl}}{m_p}\right)^3 \Rightarrow \frac{\varepsilon_\Lambda}{M_{Pl}^4} \sim \left(\frac{m_p}{M_{Pl}}\right)^6$$

↑ "АНТРОПНАЯ" ОЦЕНКА ДИККЕ

2. $\varepsilon_m \sim \varepsilon_\Lambda$, КОГДА $\frac{\delta\rho}{\rho} \sim 1$ В МАСШТАБЕ СКОПЛЕНИЙ

$$\tilde{A} \sim \Omega_{\gamma 0} \Rightarrow A^{3/4} \sim \frac{n_\gamma}{n_{CDM}} \cdot \frac{\varepsilon_\Lambda^{1/4}}{m_{CDM}}$$

Present matter content in the Universe

Multicomponent !

~ 95% of all matter not yet discovered in laboratory !

$$\Omega_a = \frac{8\pi G \varepsilon_a}{3H_0^2}$$
$$\Omega_k = -\frac{1}{a_0^2 H_0^2}$$
$$\sum_a \Omega_a + \Omega_k = 1$$

1. Usual matter
   p, n, e^-

   $\Omega_b = 0.045 \pm 0.005$

   a) BBN
   b) acoustic peaks in $\frac{\Delta T}{T}$

   $\Omega_{lum} < 0.01$ → the problem of dark baryonic matter

2. Hot dark matter
   massive neutrinos

   $10^{-3} \leq \Omega_\nu < 0.02$

   a) $P(k)$
   b) $\Delta T/T$

   $\sum_a m_{\nu a} < 1\ eV$

3. Cold dark matter
   mostly non-baryonic
   non-relativistic
   grav. clustered

   $\Omega_m = 0.27 \pm 0.04$

   a) $\Delta T/T$
   b) rotation curves
   c) LSS

4. Dark energy
   relativistic, $p < 0$, $|p| \sim \varepsilon$
   grav. unclustered

   $\Omega_{DE} = 0.73 \pm 0.04$

   a) $\Delta T/T$, $P(k)$
   b) SN Ia

Modern paradigm of the Universe evolution

$\cdots\cdots \rightarrow DS \rightarrow FRWRD \rightarrow FRWMD \rightarrow \widetilde{dS} \cdots\cdots \rightarrow$

Existense of dark energy -
- kinematical statement
assuming the "Einsteinian interpretation"

$$R_i^k - \frac{1}{2}\delta_i^k R = 8\pi G\left(T_{i\,(m)}^k + \widetilde{T}_{i\,(DE)}^k\right) \qquad 4D$$

$T_{i\,(m)}^k$ ↓ matter seen through its active gravitational mass (effect on motion of stars, galaxies and light)

Remarkably $\widetilde{T}_{i\,(DE)}^k \approx \varepsilon_{DE}\,\delta_i^k$

New (actually, very old) way of introducing the inflationary paradigm

Physical

In some period in the past, matter in the Universe was qualitatively the same as the main part of matter in the present Universe

Geometrical

Evolution of the Universe - - transition between two maximally symmetric states (space-times, in particular)

---→ De Sitter ⇒ FRW ⇒ De Sitter ---→
(RD, MD)

"Quintessence - inflaton today"

Geometrical F(R) model of dark energy

$$S = \frac{1}{16\pi G}\int F(R)\sqrt{-g}\,d^4x + S_m$$

$$F(R) = -R + f(R) \qquad R \equiv R^i_i$$

$$\frac{F}{2}\delta_i^k - F' R_i^k - (\nabla\delta_i^k - \nabla_i\nabla^k)F' = 8\pi G\, T_i^k$$

$$R_i^k - \frac{1}{2}\delta_i^k R = 8\pi G\, T_i^k +$$

$$+ \underbrace{f' R_i^k - \frac{f}{2}\delta_i^k + (\nabla\delta_i^k - \nabla_i\nabla^k)f'}_{8\pi G\, T_{i,DE}^k}$$

Particle content: graviton + massive scalar particle (called "scalaron" in A.S., 1980)

No ghosts if

① $F' < 0$ $\quad f' < 1$

② $F'' \geq 0$ $\quad f'' \geq 0$

Classically for FRW model $\begin{cases} F'(R_0) = 0 \text{ - loss of homogeneity} \\ F''(R_0) = 0 \text{ - non-analytical behaviour of } R(t) \ (R(t) = R_0 + R_1 t + R_2 t^{1/2} t + \ldots) \end{cases}$

$f(R) = R^2/6M^2$

Internally self-consistent inflationary model with a graceful exit to the subsequent FRW stage (first, MD; second, after scalaron decay, RD)

$\tau \sim \frac{M_{Pe}^2}{M^3}$ A.S., PLB (1980)

$M = 1.8 \times 10^{-6} M_{pe} \cdot \frac{60}{N}$

$n_s = 1 - \frac{2}{N} \simeq 0.97$, $2 \simeq 3 \cdot 10^{-3}$

Recent idea:

F(R) model with $F(R) \to \infty$ for $R \to 0$ as a model of dark energy at present time

Capozziello 2002
Capozziello et al. 2003
Carroll et al. 2003 ....

Main problem: effective coupling to usual matter in the Einstein frame

ОПРЕДЕЛЕНИЕ КОСМОЛОГИЧЕСКИХ ФУНКЦИЙ С ПОМОЩЬЮ ОБРАЩЕНИЯ КЛАССИЧЕСКИХ КОСМОЛОГИЧЕСКИХ ТЕСТОВ

Прямой тест	Обратный тест
$\mathcal{D}_L(z) = a_0(z_0 - z)(1+z)$	$H(z) = \left[\left(\frac{\mathcal{D}_L(z)}{1+z} \right)' \right]^{-1}$
$\theta(z) = \frac{d(1+z)}{a_0(z_0 - z)}$	$H(z) = \left[d \left(\frac{1+z}{\theta(z)} \right)' \right]^{-1}$
$\frac{dN}{dz\,d\Omega} \propto \frac{dV}{dz\,d\Omega} = f_V(z)$	$H^{-1}(z) = \frac{d}{dz} \left\{ \left(3 \int_0^z f_V(z') \cdot (1+z')^3 \, dz' \right)^{1/3} \right\}$
$f_V = a^3 (z_0 - z)^2 \left\lvert \frac{dz}{dz} \right\rvert$	
$T(z) = \int_z^\infty \frac{dz'}{(1+z') H(z')}$	$H(z) = -\left((1+z) \frac{dT}{dz} \right)^{-1}$

RECONSTRUCTION OF DARK ENERGY PROPERTIES FROM SUPERNOVA DATA

U. Alam, V. Sahni, T. D. Saini, A. S.,
astro-ph/0311364

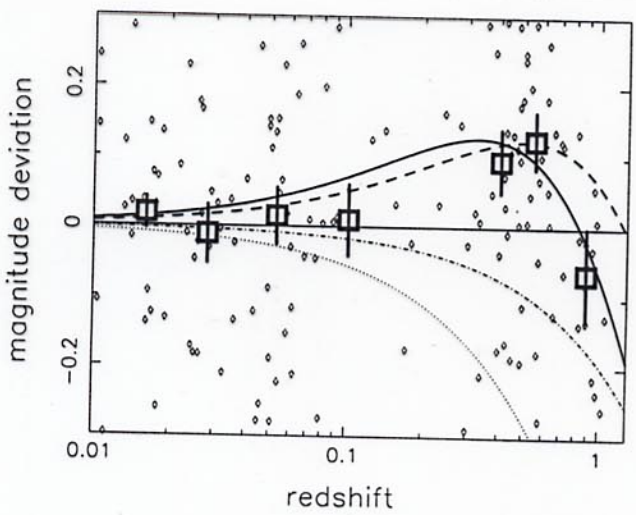

Figure 15. Literature supernovae (diamonds) shown along with median values binned by redshift (large squares). Individual points are shown without error bars for clarity. The solid horizontal line represents the empty universe with $(\Omega_{0m}, \Omega_\Lambda) = (0.0, 0.0)$. The thick solid line represents the magnitude deviation of our best-fit universe for this data-set from the empty universe. The thick dashed line represents ΛCDM with $(\Omega_{0m}, \Omega_\Lambda) = (0.3, 0.7)$, the dot-dashed and dotted lines represent cosmologies with $(\Omega_{0m}, \Omega_\Lambda) = (0.3, 0.0)$ and $(1.0, 0.0)$ respectively.

222 points total
194 points used ($z > 0.1$)

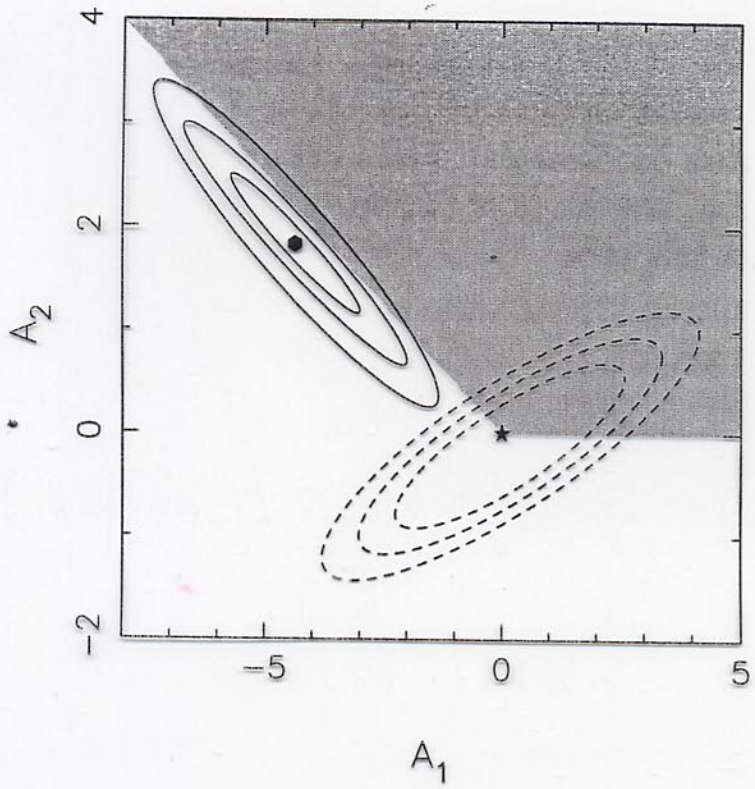

Figure 1. The (A_1, A_2) parameter space for the ansatz (7). The light grey shaded area shows the allowed region if dark energy satisfies the weak energy condition both currently and in the past: $w(z) \geqslant -1, z \geqslant 0$. The χ^2 surface has two minima, a shallow minimum at $A_1 = 0.177, A_2 = -0.119$ with $\chi^2_{\rm shallow} = 1.0402$ and a deeper minimum at $A_1 = -4.360, A_2 = 1.829$ with $\chi^2_{\rm deep} = 1.0056$. The deeper minimum is marked by a bullet. The solid contours surrounding the deeper minimum are $1\sigma, 2\sigma, 3\sigma$ contours of constant $\Delta\chi^2$ where $\Delta\chi^2 = \chi^2 - \chi^2_{\rm deep}$. Similarly the dashed contours surrounding the shallower minimum are $1\sigma, 2\sigma, 3\sigma$ contours of constant $\Delta\chi^2$ where $\Delta\chi^2 = \chi^2 - \chi^2_{\rm shallow}$. Note that the ΛCDM model (marked by a solid star) corresponds to $A_1 = A_2 = 0$ which is very close to the shallow minimum.

$$\frac{H^2(z)}{H_0^2} = A_0 + A_1(1+z) + A_2(1+z)^2 + \Omega_m(1+z)^3$$

$$A_0 + A_1 + A_2 + \Omega_m = 1$$

A. Riess et al., astro-ph/0402512

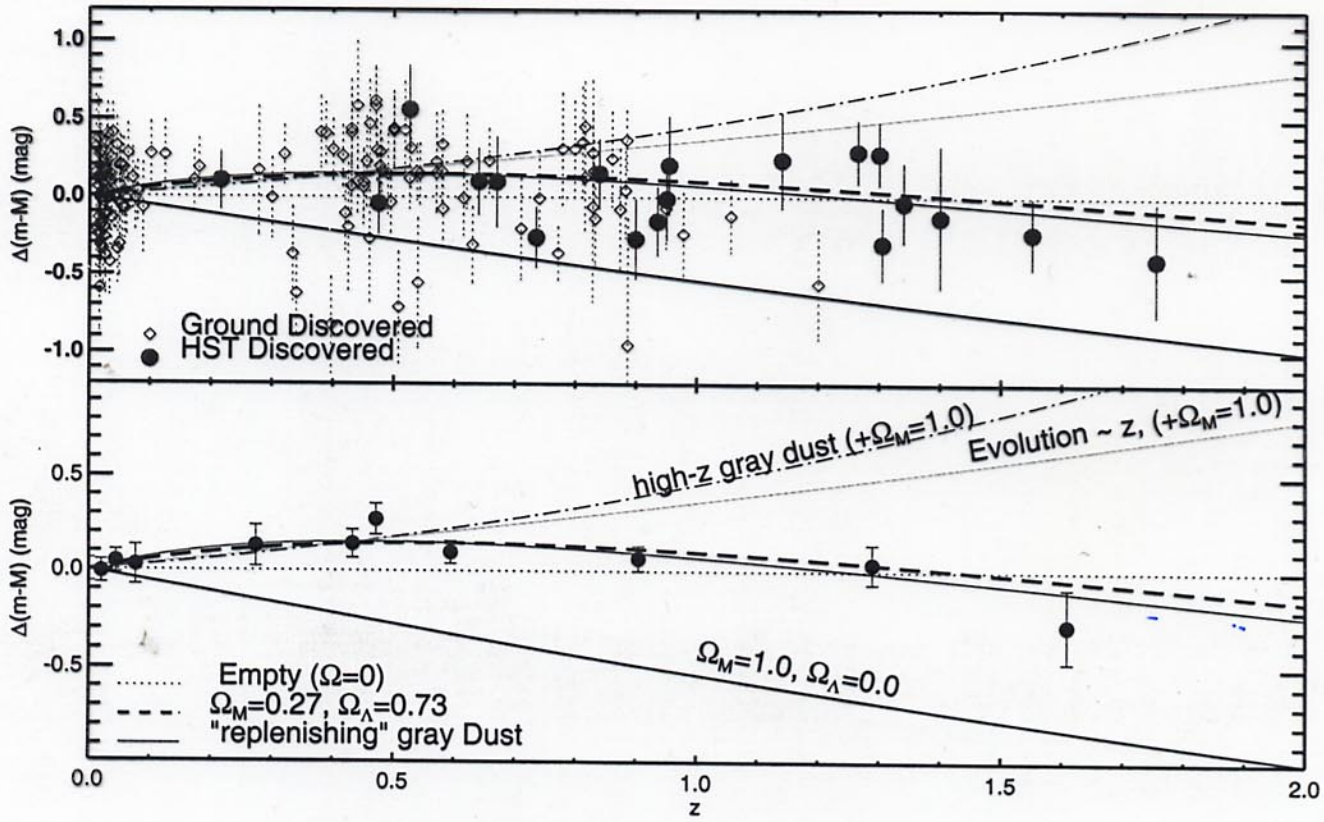

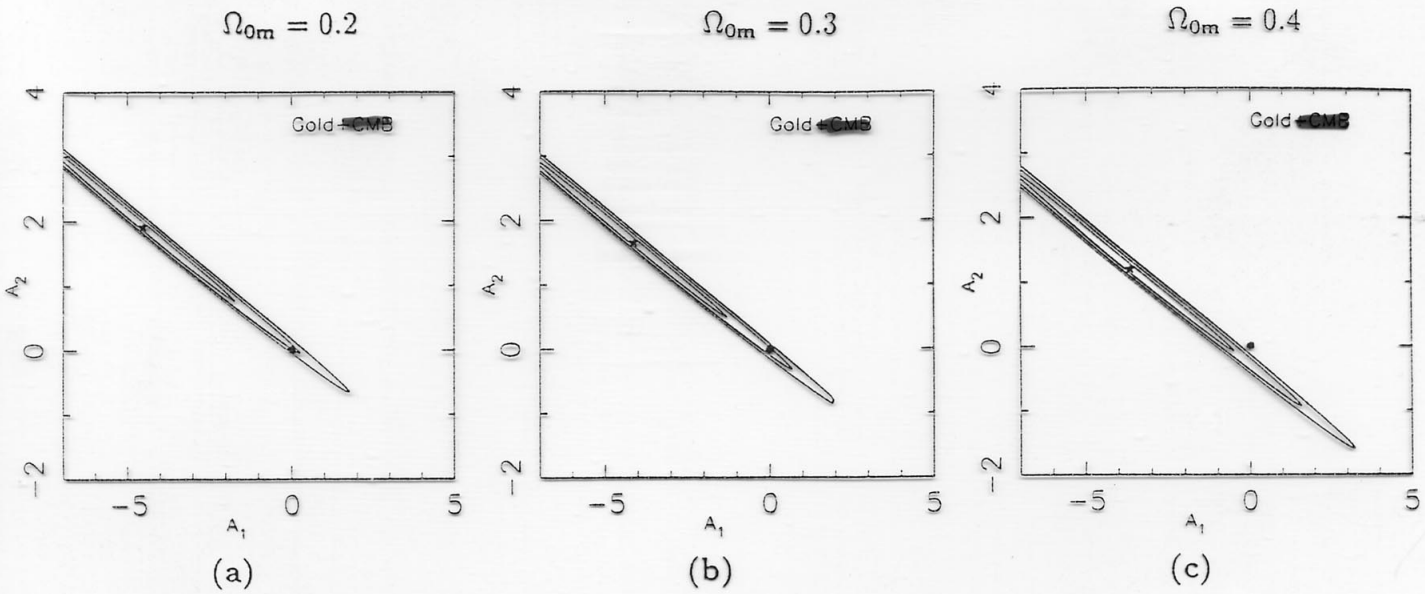

Figure 4. The (A_1, A_2) parameter space for the ansatz (5) for different values of Ω_{0m}, using the 'Gold' sample of SNe from [18]. The star in each panel marks the best-fit point, and the solid contours around it mark the $1\sigma, 2\sigma, 3\sigma$ confidence levels around it. The filled circle represents the ΛCDM point. The corresponding χ^2 for the best-fit points are given in table 1.

Table 1. χ^2 per degree of freedom for best-fit and ΛCDM models for analysis using the 'Gold' sample of SNe from [18]. w_0 is the present value of the equation of state of dark energy in best-fit models.

	Best-fit		ΛCDM
Ω_{0m}	w_0	χ^2_{min}	χ^2
0.20	−1.20	1.036	1.109
0.30	−1.35	1.034	1.053
0.40	−1.59	1.030	1.086

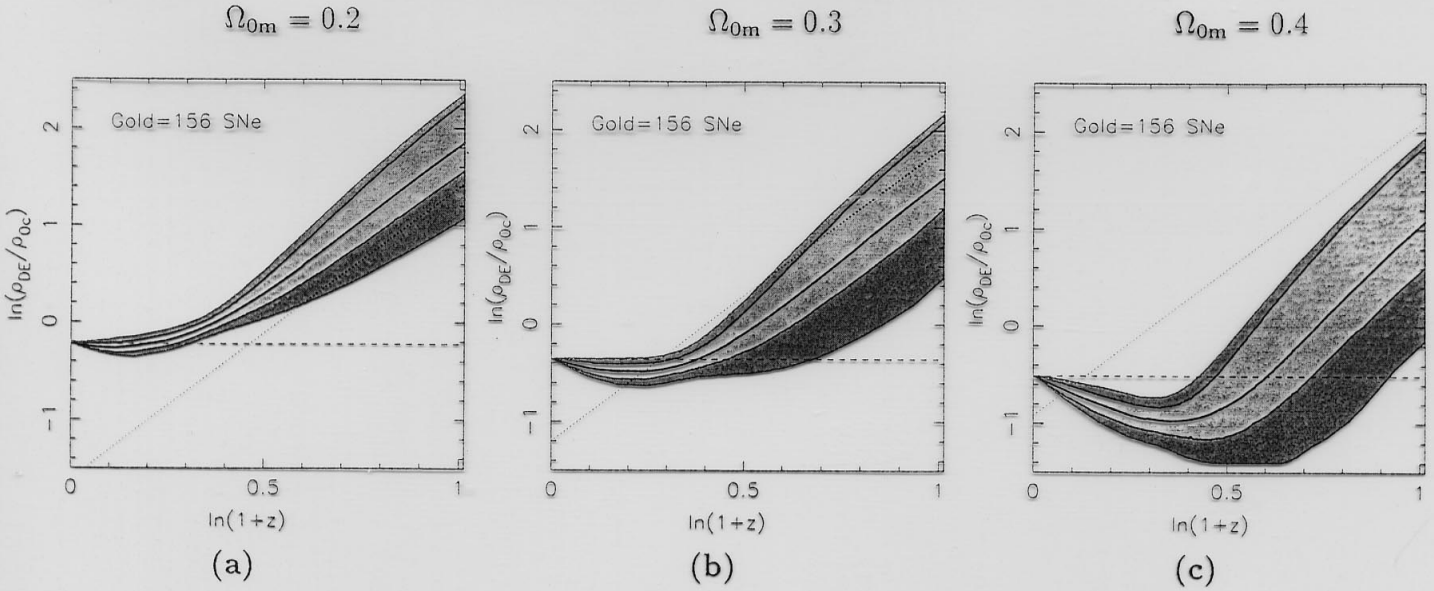

Figure 5. The logarithmic variation of dark energy density $\rho_{DE}(z)/\rho_{0c}$ (where $\rho_{0c} = 3H_0^2/8\pi G$ is the present critical energy density) with redshift for different values of Ω_{0m}, using the 'Gold' sample of SNe from [18]. The reconstruction is done using the polynomial fit to dark energy, ansatz (5). In each panel, the thick solid line shows the best-fit, the light grey contour represents the 1σ confidence level, and the dark grey contour represents the 2σ confidence level around the best-fit. The dotted line denotes matter density $\Omega_{0m}(1+z)^3$, and the dashed horizontal line denotes ΛCDM.

Table 2. The weighted average $\bar{w}$ (eq 10) over specified redshift ranges for analysis using the 'Gold' sample of SNe from [18]. The best-fit value and 1σ deviations from the best-fit are shown.

	$\bar{w}$		
Ω_{0m}	$\Delta z = 0 - 0.414$	$\Delta z = 0.414 - 1$	$\Delta z = 1 - 1.755$
0.2	$-0.847^{+0.019}_{-0.043}$	$-0.118^{+0.280}_{-0.211}$	$0.089^{+0.067}_{-0.039}$
0.3	$-1.053^{+0.089}_{-0.070}$	$-0.159^{+0.319}_{-0.259}$	$0.118^{+0.073}_{-0.041}$
0.4	$-1.310^{+0.220}_{-0.179}$	$-0.210^{+0.452}_{-0.340}$	$0.215^{+0.081}_{-0.050}$

NEXT STEP

U. Alam, V. Sahni, A. S., JCAP 0504(2004)008, astro-ph/0403687

Riess et al. 'Gold sample'
(156 SNe with z up to 1.7)
+ CMB ($R \equiv \sqrt{\Omega_{m0}}\, H_0 \int_0^{z_{rec}} \frac{dz}{H(z)} = 1.71 \pm 0.14$
from WMAP)

Conclusions

1. $\Lambda = const$ is

a) inside ~3σ with no priors on
Ω_{m0} and h

b) inside ~1σ with WMAP priors
$\Omega_{m0} = 0.27 \pm 0.04$, $h = 0.71 \pm 0.06$

2. In the case a): the best fit
$\Omega_{0m} = 0.385$, $h = 0.60$;
some noticeable evolution of w_{DE}
may exist ($w_{DE} < -1$ for $z < 0.5$
$w_{DE} > -1$ $z > 0.5$)
$z_T = 0.39 \pm 0.03$

3. In the case b):

much slower evolution, though qualitatively the same

$z_T = 0.57 \pm 0.07$

4. $\left|\frac{dw}{dz}\right| \gg 1$ is excluded → but only because of effective smoothing ($\Delta z \sim 0.3$).

$\left|\frac{dw}{dz}\right| \gg 1$ over small ranges $\Delta z \ll 1$ may not be excluded using the present data.

5. No sign of decay of Λ (increase of w at small z).

Confirming earlier results in U. Alam et al., JCAP 03(2003)001 (astro-ph/0302302)

⟷

Similar recent results:

1. Y. Wang, M. Tegmark, astro-ph/0403292
2. R.A. Daly, S.G. Djorgovski, astro-ph/0403664
3. D. Huterer, A. Cooray, astro-ph/0404062
4. Y. Gong, astro-ph/0405446

ВЫВОДЫ

1. СТАНДАРТНАЯ КОСМОЛОГИЧЕСКАЯ МОДЕЛЬ УСПЕШНО РАБОТАЕТ

2. БУДУЩЕЕ – ЗА ЕЁ РАСШИРЕНИЕМ

   а) ЗАДАЧА ДЛЯ НАБЛЮДАТЕЛЕЙ: ВЫХОД НА УРОВЕНЬ ТОЧНОСТИ 1%

   б) ЗАДАЧА ДЛЯ ТЕОРЕТИКОВ: ВЫБОР МЕЖДУ МНОГОЧИСЛЕННЫМИ ВАРИАНТАМИ ОБОБЩЕНИЯ И УНИФИКАЦИЯ КОСМОЛОГИИ

Models of dark matter

1. SUSY particles (neutralino et al.) — $m \sim 100$ GeV
2. Axion — $m \sim 10^{-5}$ eV
3. Ultra-light particles — $m \sim 10^{-23}$ eV (Gruzinov; Arbey et al. ....)
4. Brane tachyon condensate — No particle-like excitations

The latter has problems with caustics (singularities) formation (see Frolov, Kofman, A.S., hep-th/0204187; Felder, Kofman, A.S., hep-th/0208019)

Lesson: generically, theories of the $\mathcal{L} = f(\varphi, \varphi_{,m}\varphi^{,m})$ type ("k-essence, k-matter") with a non-trivial dependence on $\varphi_{,m}\varphi^{,m}$ are incomplete, further derivatives should be taken into account

Investigation of dark energy

I. From observations to theory

Reconstruction of
1) $H(z)$, $\varepsilon_{DE}(z)$
2) $q(z)$, $P_{DE}(z)$, $w_{DE}(z)$
3) $r(z)$, $\frac{dw_{DE}}{dz}$

1. Inversion of classical cosmological tests
2. CMB (acoustic peaks spacing, ISW)
3. $\left(\frac{\delta\rho}{\rho}\right)_m(z)$, $\Phi(z)$ from gravitational lensing, correlation of $\frac{\delta\rho}{\rho}$ with ISW

II. From theory to observations

Models (many of them!)

1. Fundamental constant
2. Scalar field (with $m \sim 10^{-33}$ eV)
3. Geometrical dark energy